

---

# Automatic Generation of Camera Motion to Track a Moving Guide

Onno Goemans and Mark Overmars

Institute of Information and Computing Sciences, Utrecht University,  
P.P. Box 80.089, 3508 TB Utrecht, The Netherlands.  
Email: [onno,markov]@cs.uu.nl.

**Abstract.** Following a moving object through a cluttered virtual environment can be a challenge for a user. Instead one would prefer to concentrate on observing the object and its environment. In this paper we propose an approach to automatically generate a camera motion, such that the user maintains visibility with an object moving along a known path through a virtual environment. The user specifies the camera placement at the start and end of the object path, and the constraints on the camera placement relative to the object. The system then computes a smooth camera path, satisfying the constraints. The approach first applies a single-shot probabilistic road map technique to generate an initial camera path. Several optimizations are proposed to speed up the construction considerably. The initial path is then smoothened to present the user a pleasant camera motion. The approach has been implemented and tested. It is fast and computes paths in complicated 2D and 3D environments in less than a second.

## 1 Introduction

A growing public is coming into contact with virtual environments as a result of the combination of faster and cheaper 3D graphics technology and the increasing use of broadband internet connections. Crucial in all virtual environment applications is effective control of the user's viewpoint, or virtual camera. For the novice user, navigating a virtual camera through an environment can be challenging. Such a challenge can easily become overwhelming when the user has to perform a task within a certain time frame. A typical task is following a guide object that is moving through the virtual environment.

In this paper, we propose a technique which generates a camera motion to track a guide (object). We assume the guide moves along a known path through a given virtual environment. The user specifies the placement of the camera at the start and end of the guide path, and constraints on the camera placement relative to the guide. The resulting camera motion must satisfy the user's constraints, and the camera must at all times maintain visibility with the guide; see Fig. 1(a) and (b).

The last decade, much research has been done to assist the user in controlling the camera [9,13,14,22,26] and to control the camera automatically. We can roughly divide the latter research into three groups of techniques.

The first group consists of techniques that plan camera motion as a sequence of shots. The shots are either based on cinematographic rules [6,15] or calculated by solving a set of constraints [2,8,11]. The second group consists of techniques that generate a collision free camera motion from a start to a goal placement through a virtual environment [4,7,23,24]. The third group consists of techniques that generate a camera motion to track a moving guide. Most of these techniques assume the path of the guide to be unknown [10,12]. None of these techniques are suitable to solve our problem: when the guide path is unknown, a smooth motion maintaining visibility is not always possible.

LaVall *et al.* [18] proposed an approach that describes the target path as a sequence of configurations in a two-dimensional environment. For each of these configurations the approach determines the visibility region, which it then uses to calculate an optimal path. We expect that the visibility region approach is not viable in a three-dimensional environment because of the large computation time.

Li *et al.* assumed the guide path to be known; they proposed an approach to plan a camera motion through a two-dimensional environment [20,21]. Their approach maintains visibility at all time and optimizes several additional camera-specific criteria. They described a camera configuration as the position relative to a guide position, and a guide position as the position of the guide on the predefined guide path at a point in time. The continuous space containing all camera configurations is approximated with a uniform grid of configurations. The approach applies a best-first planning algorithm to find a collision-free camera path in this configuration-time space. Their approach is limited to two-dimensional environments that are not too complicated as otherwise the grid becomes too large. Li *et al.*'s approach inspired our representation for camera configuration, but we use a different planning approach that can also be used in large three-dimensional environments.

Our aim is to efficiently solve the given problem for two-dimensional as well as three-dimensional environments. The general idea is as follows. The configuration space describes all possible placement combinations of camera and guide. The relevant subspace contains all configurations that satisfy the constraint that the camera maintains visibility with the guide, and the constraints on the camera placement relative to the guide. We apply a single-shot probabilistic road map method, or PRM [1,3,16,17,25], to construct a road map in this relevant subspace. We considerably improve its efficiency by focusing on "useful" road map growth. A valid camera motion is found once the road map connects the start and goal configuration. We then smooth this initial camera motion to eliminate unnecessary camera movement.

The paper is structured as follows. The first four sections address the problem in a two-dimensional workspace. Section 2 discusses the guide, camera, and configuration space in more detail. Section 3 describes the basic approach to generate the initial camera path, and then discusses two improvements. Section 4 discusses the application we built to test the approach, provides test results, and explains the automation of a PRM-parameter. The

technique is able to solve complex test cases within one second. Section 5 discusses the smoothing of the initial camera path. Section 6 describes the extension of the motion planner to 3D environments. The generalization is almost straight-forward and solutions are found equally fast.

## 2 Preliminaries

For the moment we assume that the guide and camera move in a two-dimensional environment. We specify a guide placement  $g$  with three parameters: two for its position  $\mathcal{W}(g)$  in the workspace, and one for its orientation. The guide moves along a known path  $\mathcal{GP}$  through the workspace. The *length offset*  $lo$  is the normalized length along  $\mathcal{GP}$  between the start configuration of  $\mathcal{GP}$  and configuration  $g \in \mathcal{GP}$ . The guide path is defined as a mapping from length offset to guide configuration; e.g.  $\mathcal{GP}(0)$  and  $\mathcal{GP}(1)$  uniquely identify the start and end configuration of  $\mathcal{GP}$ .

As proposed by Li *et al.* [20,21], we specify the camera configuration  $v$  relative to a given guide configuration  $g$ . The *tracking distance* is the Euclidean distance between  $v$  and  $g$  in the workspace; and the *tracking angle* is the orientation of the vector  $\overrightarrow{\mathcal{W}(g)\mathcal{W}(v)}$  in the workspace. We choose the camera orientation such that the camera always looks straight at the guide. Length offset, tracking distance and tracking angle together uniquely define the position and orientation of the camera. See figure 1(c).

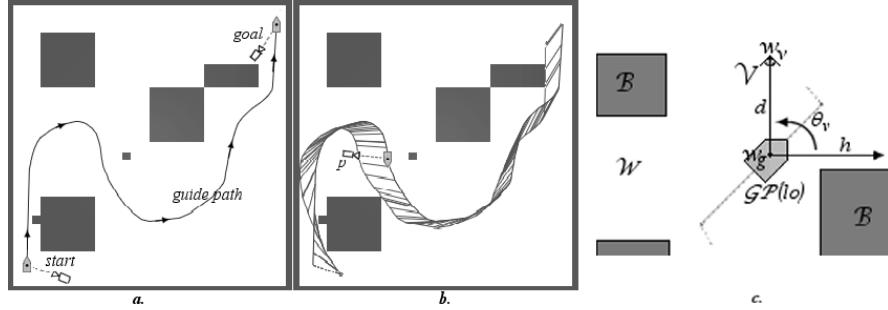


**Fig. 1.** Figure (a) depicts the guide path; at the start and end the camera placements are shown. Figure (b) shows a possible camera path from the start to the goal. In figure (c) the camera configuration  $v$  is defined relative to guide configuration  $\mathcal{GP}(lo)$  by tracking distance  $d$  and tracking angle  $\theta_v$ .

We refer to the imaginary line segment connecting the camera and the guide as the *viewing line*. Recall that the user defines constraints on the camera placement relative to the guide. These constraints are a minimum and maximum on the tracking distance, and a minimum and maximum on the tracking angle. Note that the constraints on the tracking angle are specified

relative to the guide orientation. Thus if the guide orientation changes then the allowed tracking angle range changes as well.

Let us now look at the configuration space in which we will solve our motion planning problem. A configuration describes a combined placement of guide and camera. That is, a guide configuration on the guide path, and a camera configuration relative to this guide configuration. We specify such a configuration with two parameters: the length offset  $lo$ , which specifies the guide configuration, and the tracking angle  $ta$ , which describes the camera configuration relative to  $\mathcal{GP}(lo)$ . The configuration description does not contain the tracking distance, because we fix the tracking distance at its user-defined minimum. The motivation for this choice is that if no solution exists for the minimum tracking distance, then no solution exists at all. The actual tracking distance can easily be computed during a post-processing phase. We refer to the configuration space as the *configuration-length offset space*, or  $\mathcal{CLO}$ -space. A path through the  $\mathcal{CLO}$ -space is a *camera path*.

Not all  $\mathcal{CLO}$ -configurations are valid, because of the visibility constraint and the user's constraints on the tracking angle. We refer to the valid part of the  $\mathcal{CLO}$ -space as *free  $\mathcal{CLO}$ -space*, or  $\mathcal{CLO}_f$ . See figure 2.

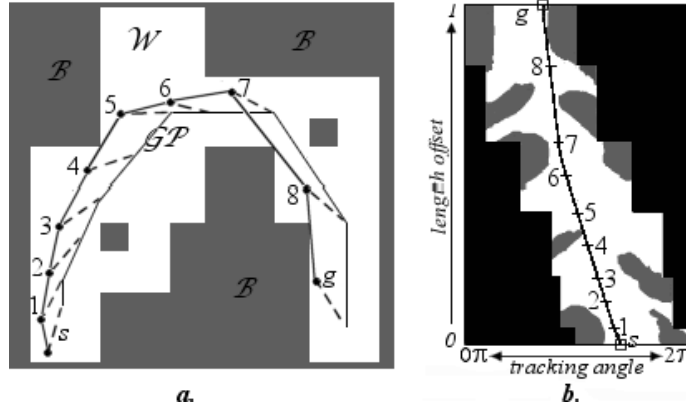


**Fig. 2.** Figure (a) shows a workspace, where the sequence of line segments tagged with  $\mathcal{GP}$  is the guide path. Configurations  $s$  and  $g$  are the start and goal configuration. The sequence of line segments tagged with numbers is the camera path, where the dotted lines illustrate how the camera looks at the guide. Figure (b) shows the  $\mathcal{CLO}$ -space. The white area is the  $\mathcal{CLO}_f$ -space. The gray areas illustrate the collection of occluded configurations. The black areas illustrate the collection of configurations not allowed because of the tracking angle constraints. The line through  $\mathcal{CLO}_f$  is the path connecting the start and goal configuration, and corresponds to the camera path in the workspace (figure 2a)

We assume that the guide only moves forwards along its path, and that the camera only moves when the guide moves. Consequently, a path through the  $\mathcal{CLO}$ -space must be increasingly monotone in the length offset direction. A camera path is free if it lies entirely in the  $\mathcal{CLO}_f$  space; which means that the viewing line never intersects any obstacles in the workspace. See figure 2.

### 3 Motion planner

The user specifies the start configuration  $clo_{start}$  and goal configuration  $clo_{goal}$ , which are respectively at length offset 0 and 1. Now the goal of the motion planner is to generate a free camera path  $P_{solution}$ , which connects  $clo_{start}$  and  $clo_{goal}$ . We apply a single-shot motion planner based on the PRM-approach to construct a graph  $G = (V, E)$ , or road map, in the  $\mathcal{CLO}_f$ -space. The graph nodes  $V$  correspond to free configurations, and edges  $E$  to free paths. Recall that a path in the  $\mathcal{CLO}$ -space must be monotone in length offset. This restriction imposes two limitations on the graph: firstly,  $G$  is a directed graph; and secondly, for all edges the length offset of the begin configuration must be smaller than the length offset of the end configuration.

The start and goal configuration are the first two nodes added to the graph. Next the motion planner first chooses a random free configuration  $clo_{new}$  and adds it to the graph; then the motion planner attempts to connect  $clo_{new}$  to the graph by connecting  $clo_{new}$  to nearby nodes (*neighbors*); and finally the motion planner checks whether the graph connects  $clo_{start}$  and  $clo_{goal}$ . These last three steps are repeated in a loop, referred to as the PRM-loop, until  $P_{solution}$  is found.

---

#### Algorithm 1 Overview Motion Planner

1.  $E \leftarrow \emptyset$  [edges]
  2.  $V \leftarrow \{clo_{start}, clo_{goal}\}$  [nodes]
  3. **loop**
  4.    $clo \leftarrow \text{randomly chosen configuration} \in \mathcal{CLO}_f$  [Sampling]
  5.    $N_{clo} \leftarrow \text{set of neighbors of } clo \text{ chosen from } V$  [Neighbor set]
  6.   Attempt to connect  $clo$  to its neighbours [Connection]
  7.   **if**  $G$  connects  $clo_{start}$  and  $clo_{goal}$  **then** return path [Termination]
  8.   **else** continue loop
- 

#### 3.1 Basic motion planner

We need to fill in some details in the basic planner:

**Sampling:** The motion planner picks a random configuration  $clo_{new}$  from  $\mathcal{CLO}$ . If the random configuration is free, then the motion planner adds  $clo_{new}$  to  $V$ . The motion planner repeats the sampling, if  $clo_{new}$  is not free.

**Neighbor set:** The planner selects the nodes  $\in V$  that are within a certain length offset range from  $clo_{new}$ 's length offset. This length offset range is referred to as the *neighbor set distance*. Subsection 4.2 further discusses the choice of neighbor set distance.

**Connection:** Next the algorithm attempts to connect  $clo_{new}$  to each of its neighbors with a *local path* computed by the *local planner*. A local path is the shortest possible path between two configurations in the  $\mathcal{CLO}$ -space. If a local path is occlusion free, then it is added as an edge to the road map.

**Termination:** The algorithm first checks if  $clo_{start}$  and  $clo_{goal}$  are in the same connected graph component. If this test is positive, then the directed graph is queried to determine whether  $G$  connects  $clo_{start}$  and  $clo_{goal}$ . If  $G$  connects the start and goal configuration, then the algorithm returns  $P_{solution}$ ; otherwise the PRM-loop is repeated.

### 3.2 “Push” sampling

A narrow passage in the  $\mathcal{CLO}_f$ -space is a length offset interval for which a relatively small part of the tracking angle interval consists of free configurations. The chance that the sampler randomly generates a free sample in an area of the  $\mathcal{CLO}_f$ -space is determined by the size of the area. Eventually enough samples will be generated in a narrow passage to enable the generation of a path through the passage; however, this process will be rather time-expensive.

To increase the sample generation in narrow passages, the “push” motion planner pushes a new sample out of the obstacle in case of occlusion; as has also been suggested for PRM application in other motion planning problems [1,25]. The pushing is done by changing the tracking angle value while maintaining the same length offset. Thus the narrower a passage, the higher the expected number of nodes in the passage.

### 3.3 “Useful” nodes

Occlusion checks require collision tests, which takes up more than 90% of the motion planner’s execution time. Hence the motion planner should avoid occlusion checks whenever possible. This subsection discusses the concept of usefulness in the framework of our study. We first experimented with growing trees [19] to reduce useless roadmap growth; however the gain was only marginal. Due to the monotonicity property, the roadmap graph  $G$  is a directed acyclic graph. We exploit this roadmap property; as a result the performance of the motion planner improves drastically.

Let  $v$  be a node in  $G$ . We refer to the nodes that connect to  $v$  as the *ancestors* of  $v$ ; and the nodes to which  $v$  connects as *descendants* of  $v$ . We define the length of a path  $P$  as the difference in length offset between  $P$ 's

start and goal configuration. Now let  $av$  be the ancestor of  $v$  with the smallest length offset; and let  $dv$  be the descendant of  $v$  with the largest length offset. The camera path  $P(av, dv)$  is the longest path (in the graph) of which  $v$  is a node. If  $v$  is not connected to any ancestors and descendants, then the longest path consists only of node  $v$ . We denote the longest path containing  $v$  by  $\hat{P}(v)$ . See figure 3(a).

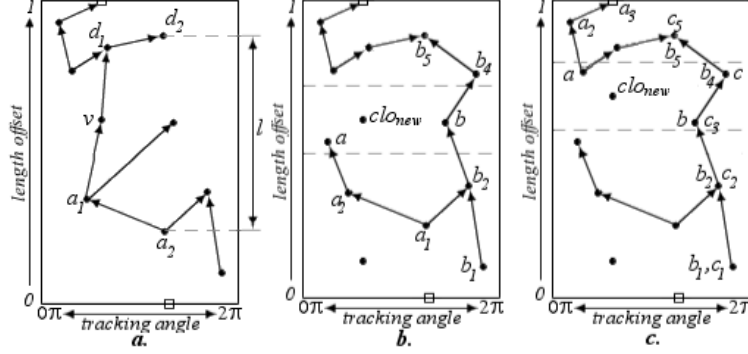


**Fig. 3.** Figure (a): The set of ancestors and descendants of node  $v$  are respectively  $\{a_1, a_2\}$  and  $\{d_1, d_2\}$ . The longest path  $\hat{P}(v)$  is  $P(a_2, d_2)$  with length  $l$ .

For each graph-node  $v$  we store a  $\hat{P}$ -record, which describes  $\hat{P}(v)$ . The record stores the length offsets of  $\hat{P}(v)$ 's begin and end configuration, which are respectively referred to as  $\hat{P}^0(v)$  and  $\hat{P}^1(v)$ . Thus for example  $\hat{P}^0(v)$  in figure 3(a) is the length offset of node  $a_2$ .

To describe the usefulness-criterion, we first introduce an alternative description of the motion planner's goal. Recall that the motion planner expands the road map until a path is found. The length offsets of  $clo_{start}$  and  $clo_{goal}$  are respectively 0 and 1, hence the length of  $P_{solution}$  is 1. All other paths of the road map are shorter. Thus we can redefine the goal of the motion planner as the creation a path of length 1. In other words, the motion planner expands the road map until  $\hat{P}$  of one of its nodes is of length 1.

Now let us return to the criterion of usefulness. Recall that the PRM-loop starts with the generation of a new sample  $clo_{new}$ . The next step is the generation of the neighbor set containing all nodes close to  $clo_{new}$ . One of the three following scenarios occurs after the neighbor set generation: In the first scenario the neighbor set is empty. In the second scenario, the motion planner can connect  $clo_{new}$  to the road map such that  $\hat{P}(clo_{new})$  is potentially longer than the longest path of any of its neighbors; see figure 3(c): if  $clo_{new}$  is successfully connected to neighbors  $a$  and  $b$ , then the longest path  $\hat{P}(clo_{new})$  is longer than  $\hat{P}(a)$  and  $\hat{P}(b)$ . In the third scenario  $\hat{P}(clo_{new})$  does not exceed the length of the longest path of one of its neighbors; see figure 3(b): even if  $clo_{new}$  is successfully connected to neighbors  $a$  and  $b$ , the longest path

$\hat{P}(clo_{new})$  can clearly not become longer than  $\hat{P}(b)$ . The sample  $clo_{new}$  is called useful when one of the first two scenarios occur. We will only add useful nodes. It can be proven that this approach is probabilistically complete.

Once it is decided that the addition of  $clo_{new}$  is useful, the next step is to connect  $clo_{new}$  to the roadmap by adding edges. The addition of an edge is only useful, when it increases the length of the current  $\hat{P}(clo_{new})$ . Let us fill in the details:

**Sampling:** We can use the basic sampler or the push sampler to generate  $clo_{new}$ . The difference is that the motion planner does not perform an occlusion check  $clo_{new}$  before  $clo_{new}$  is found to be useful.

**Neighbor set generation:** The motion planner again compiles the neighbor set  $N_{clo}$  by taking all nodes  $\in V$  within a certain length offset range from  $clo_{new}$ . We refer to neighbors with a smaller length offset than  $clo_{new}$  as *backward neighbors*; and neighbors with a larger length offset than  $clo_{new}$  as *forward neighbors*. We now determine whether  $clo_{new}$  is a potentially useful node. If not,  $clo_{new}$  is discarded and the PRM-loop is repeated.

A longest path of road map node  $v$  can be divided in two sub paths. The first sub path consists of  $v$  and the ancestors of  $v$ ; and the second sub path consists of  $v$  and descendants of  $v$ . With this division in mind, we can break the construction of  $\hat{P}(clo_{new})$  in two parts as well: the connection of a backward neighbor  $bn$  to  $clo_{new}$ , where  $\hat{P}^0(bn)$  should be as small as possible; and the connection of  $clo_{new}$  to a forward neighbor  $fn$ , where  $\hat{P}^1(fn)$  should be as large as possible.

The motion planner splits the neighbor set  $N_{clo}$  into the set of backward neighbors  $BN_{clo}$ , and the set of forward neighbors  $FN_{clo}$ . The nodes of the first set are sorted on increasing  $\hat{P}_0$  value, and the elements of the latter on decreasing  $\hat{P}^1$  value. See figure 4. So we first try the connections that will lead to the longest paths.

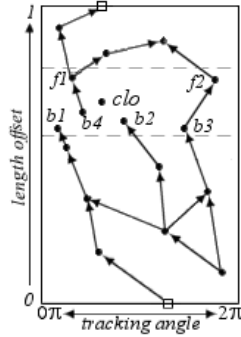


**Fig. 4.** The sorted backward neighbors set  $BN_{clo}$  is  $\{b1, b2, b3, b4\}$  and the sorted forward neighbour set is  $\{f1, f2\}$ .



**Connection:** The motion planner attempts to connect the backward neighbors to  $clo_{new}$ , starting with the first element of  $BN_{clo}$ . This connection process continuous until the local planner generates a free local path, or until all backward neighbors are tested and the corresponding local paths are all found occluded. In the first case the motion planner sets  $\hat{P}^0(clo_{new})$  as  $\hat{P}^0(nb)$ ; otherwise  $\hat{P}^0(clo_{new})$  is set to  $clo_{new}$ . Similarly, the motion planner attempts to connect  $clo_{new}$  to a forward neighbor, and sets  $\hat{P}^1(clo_{new})$  accordingly. Again in case of failure  $\hat{P}^1(clo_{new})$  is  $clo_{new}$ . This approach reduces the number of attempted connections considerably.

Once  $clo_{new}$  is connected to the graph, the  $\hat{P}$ -records of  $clo_{new}$ 's ancestors and descendants must be updated:  $\hat{P}^0(clo_{new})$  is propagated through  $clo_{new}$ 's ancestors, and  $\hat{P}^1(clo_{new})$  is propagated through  $clo_{new}$ 's descendants.

**Termination criterion:** The goal of the motion planner is to construct a longest path of length 1. This is the case once the length of  $\hat{P}(clo_{new})$  is 1.

## 4 Experimental results

We implemented the techniques described above in C++. As collision check package we used Solid [5]. All tests are run on a computer with a 2.4 GHz Pentium 4 processor, 512 MB of memory and Windows XP operating system.

### 4.1 Results

Figure 5, 6 and 7 illustrate the test cases. Each left picture depicts the workspace containing the guide path, and the start and goal camera configuration at respectively the start and end of the guide path. Each right picture shows a possible camera path. In all experiments we use a maximal tracking angle of  $\pi/2$ ; that is, the camera must stay behind the guide.

We use test case 1 to test the motion planner in an environment with a rather uniform obstacle distribution, and enough room for the camera to maneuver. The purpose of test case 2 is to determine the effect of the number of guide path segments on the planner's efficiency. The path is short, but consists of a large number of small segments, increasing the cost of the local planner. Case 3 tests the planner's capability to operate in cluttered environments with a challenging guide path. Below you find the results of the basic planner, the "pusher" planner and the "useful" planner equipped with the push sampling. Recall that the tracking distance is fixed at the most challenging value. The results, expressed in seconds, are averages over 250 runs.

	Test case 1	Test case 2	Test case 3
Basic planner	1.29	1.02	60+
Push planner	0.91	0.31	45.96
Push + Useful planner	0.22	0.02	0.60

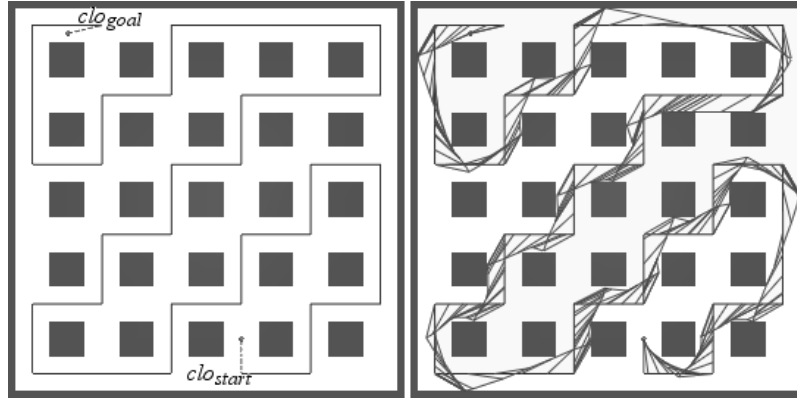


Fig. 5. Test case 1

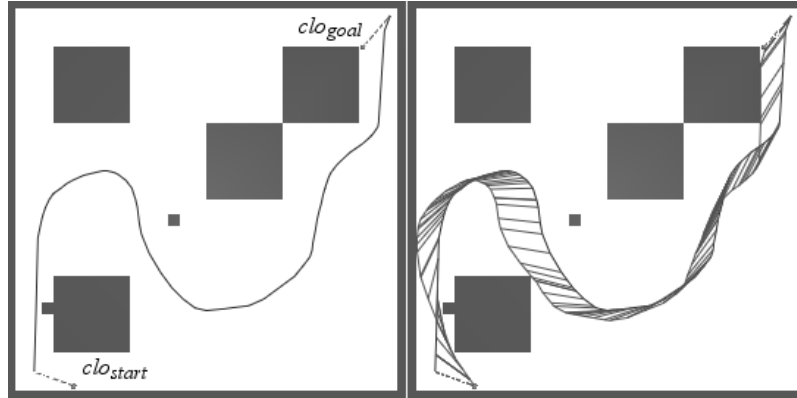


Fig. 6. Test case 2

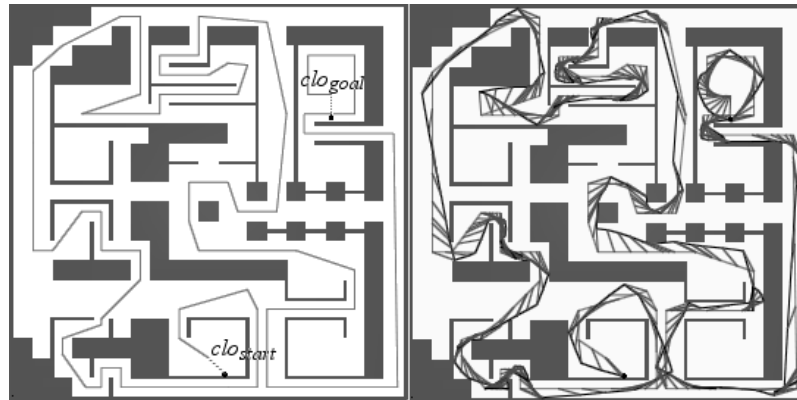


Fig. 7. Test case 3

The basic motion planner solves test case 1 and 2 in about one second. However the basic planner is not able to solve the complex test case 3 within a minute. To give an impression of the road map size: for test case 3, the road map on average consisted of about 60,000 edges and 1,600 nodes.

The "pusher" motion planner clearly performs better overall, although its performance in test case 3 is still not satisfying. For test case 3, the road map now consisted of about 43,000 edges and 1,400 nodes.

Adding the usefulness test solved each test case well within a second. The notion of usefulness enables the motion planner to quickly expand the road map in uncluttered areas of the  $\mathcal{CLO}$ -space; and then focus on the cluttered areas of the  $\mathcal{CLO}$ -space, while discarding the already covered easy areas. The roadmap of test case 3 now consists on average of only about 600 edges and 400 nodes.

## 4.2 Neighbor Set Distance

There is one parameter to fill in; the neighbor set distance ( $nsd$ ). For practical use it is important that the system determines this value automatically. This subsection describes a technique we refer to as  $NSD_{auto}$ .

Let us first define a few roadmap properties. The percentage of all local paths that is tested occlusion free, is referred to as the *success ratio*. Furthermore, the percentage of the length offset interval covered by the road map  $G$  is denoted as the *coverage ratio*.

$NSD_{auto}$  consists of two phases. In the first phase, the learning phase, the road map provides too little and too unreliable information to base  $nsd$  on. Hence in the learning phase  $nsd$  is a constant value. Experiments in a variety of scenes show that the constant  $nsd$  is rather scene independent; somewhere in the range from 0.05 to 0.10 is optimal. The  $NSD_{auto}$  goes into the next phase, when the coverage ratio becomes larger than the success ratio. This transition assures on the one hand that the motion planner "learns" enough about the environment, and on the other that the motion planner's efficiency does not decrease because of the relatively large constant  $nsd$ . During the second phase, we base  $nsd$  on the average length of the last  $c$  free local paths. Experiments show that the results are optimal when  $c$  is between about 25 and 100. For test cases of average complexity,  $NSD_{auto}$  spends most of its time in the second phase.

The  $NSD_{auto}$  as described above causes two undesired side effects, which result in a decrease of the motion planner's performance. Both problems are caused by the decrease of  $nsd$  over time and can easily be solved. One problem occurs when the neighbor set of a new sample  $clo_{new}$  is empty. Figure 8 illustrates the problem: The neighbor set  $N$  of the newly generated sample  $clo$  is empty; thus the motion planner would mark  $clo$  as useful, and add  $clo$  to the roadmap. However the addition of  $clo$  is not useful, since the graph already spans the  $\mathcal{CLO}$ -space covered by the neighbor set  $N$ . Note that this situation does not occur when we use a fixed  $nsd$ , since in that case either

node  $v$  or  $w$  would be in  $N$ . To eliminate this problem, the motion planner determines whether the graph already covers the neighbor set length offset interval. If so, then the addition of  $clo_{new}$  is considered not useful.

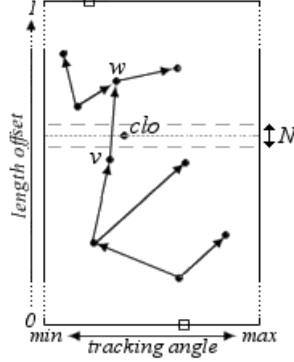


**Fig. 8.** Illustration of problem occurring because of decreasing  $nsd$

The second problem occurs when  $nsd$  has become small, while a relatively long local path is needed to bridge a gap in the road map. We solve this problem by setting a lower boundary for  $nsd$ ; which we base on the tracking distance.

Experiments show that the motion planner performs as well with  $NSD_{auto}$  as when the neighbor set distance is manually optimized. The results in the previous section were obtained using  $NSD_{auto}$ .

## 5 Smoothing

Path quality indicates how pleasant the camera images are to watch for a user. The motion planner as described so far disregards this aspect. See figure 9(a). Experiments show that the path quality is inversely related to the total tracking angle change. Hence to improve the path quality, the motion planner has to minimize the total tracking angle change. This smoothing process consists of two phases.

The first phase is active while the motion planner generates the initial camera path: The weight of each road map edge  $e$  is the tracking angle difference between  $e$ 's begin and end configuration. When  $clo_{start}$  and  $clo_{goal}$  are graph connected, the path with the smallest total weight is taken as initial solution  $P_{solution}$ .

The second phase applies a standard smoothing approach [24]. The motion planner repeatedly replaces random path segments of  $P_{solution}$  with new path segments of higher quality using the local planner; and in doing so increases the overall quality of  $P_{solution}$ .

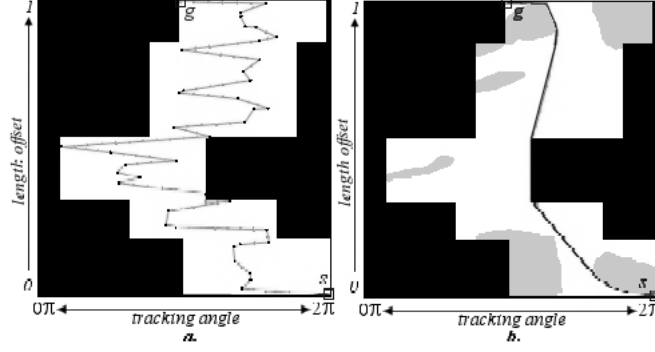


**Fig. 9.** Figure (a): A typical example of an unsmooth camera path in the configuration space. The resulting camera images are unpleasant to watch, because the camera changes its tracking angle frequently. Figure (b): The white area is an approximation of  $\mathcal{CCO}_f$ . The path is an example of a smoothed path.

The longer this is repeated, the smoother  $P_{solution}$  becomes. Figure 9(b) illustrates a smoothed path for the example test case. Without smoothing the motion planner generates  $P_{solution}$  for the example test case on average in 0.1 second. The (close to) optimally smoothed path as illustrated in figure 9 is on average generated in 0.5 second. Experiments show however that optimal smoothing is not necessary to ensure a satisfying path quality: the motion planner generates a satisfying smooth  $P_{solution}$  in on average 0.2 second. The three test cases described in the previous section are all solved and smoothed within a second. We expect that the smoothing phase can easily be improved to reduce its execution time even further.

## 6 3D Motion Planner

We so far discussed camera motion generation in a two-dimensional workspace. A virtual environment however is three-dimensional and the motions of the guide and camera are not always reducible to a two-dimensional plane. The motion planner described in the previous sections though is easily extendable to operate efficiently in a three-dimensional workspace. We briefly describe the required changes here.

The guide path remains a map from length offset to guide configuration, where the guide configurations are now described by six parameters. Recall that the camera position is specified relative to a guide configuration. In the two-dimensional workspace we needed the tracking distance and the tracking angle to describe this relative position. In the three-dimensional situation we add a second tracking angle to describe the relative vertical angle. The camera orientation is again discarded: the camera will always look straight at the guide; furthermore, the camera's up-vector is kept equal to the guide's up-vector. The corresponding  $\mathcal{CCO}$ -space is a three-dimensional space spanned

by both tracking angles and the length offset. The motion planner works without adaptation on the expanded  $\mathcal{CLO}$ -space. We implemented and tested the three-dimensional motion planner. The “push” and “usefulness” techniques again result in a drastic performance improvement.

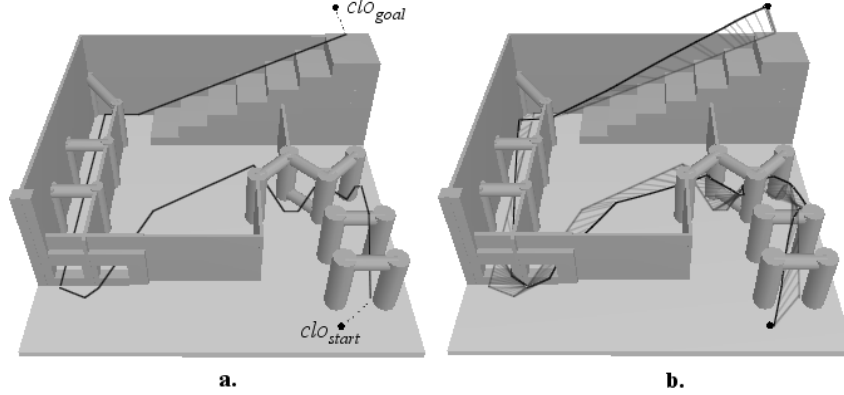


**Fig. 10.** Figure (a) shows the guide path, and the start and goal configurations of the camera as  $clo_{start}$  and  $clo_{goal}$ . Figure (b) shows the guide path in gray and camera path in black. The short lines between the guide and camera path illustrate viewing directions of the camera.

Figure 10 shows a typical three-dimensional test case with open spaces, narrow passages and height variations. As for the two-dimensional test cases, the motion planner generates a smooth camera path in less than a second. The resulting roadmap again is relatively small: on average it contains about 150 edges and 100 nodes.

## 7 Conclusion

We presented a technique to generate a camera motion such that the camera tracks a guide moving through a known environment along a known path. The motion planner applies a single-shot PRM approach to construct a graph in the free configuration space. A substantial performance gain is accomplished by a new technique, which determines whether a node or edge should be added to the road map based on its usefulness. The resulting camera path is smoothened to improve the path quality. Experiments show that the planner can operate in three-dimensional environments, and provide the user with a fast responds as is needed for interactive environments.

A number of extensions are possible. When the guide is an object rather than a point, we might want to enforce the camera to see the complete guide (and even some part around it). This can easily be achieved by replacing the

occlusion check by an intersection test with a visibility cone. We can also easily deal with preferred tracking angles by changing the sampling distribution and the smoothing process. Preferred tracking distance can be achieved in a post processing stage. Finally, additional camera motion properties such as camera speed, camera acceleration, changes in tracking distance and changes in the camera orientation can be incorporated using techniques similar to those proposed in [24].

**Acknowledgement** This work was partly supported by the Netherlands organization for Scientific Research (NWO), and by the IST Programme of the EU as a Shared-cost RTD (FET Open) Project under Contract No IST-2001-39250 (MOVIE - Motion Planning in Virtual Environments).

## References

1. N. Amato, Y. Wu (1996). “*A randomized roadmap method for path and manipulation planning*”. Proc. IEEE Int. Conf. on Robotics and Automation, 1996, pp. 113-120.
2. W.H. Bares, S. Thainimit, S. McDermott (2000). “*A model for constraint-based camera planning*”. Smart Graphics. Papers from the 2000 AAAI Spring Symposium (Stanford, March 20-22, 2000), pages 84-91, Menlo Park, 2000. AAAI Press.
3. J. Barraquand, L. Kavraki, J.-C. Latombe, T.-Y. Li, R. Motwani, P. Raghavan (1997). “*A random sampling scheme for path planning*”. Int. Journal of Robotics Research 16 (1997), pp. 759-774.
4. S. Beckhaus, F. Ritter, T. Strothotte (2000). “*Cubicalpath – Dynamic Potential Fields for Guided Exploration in Virtual Environments*”. roceedings Pacific Graphics 2000 (Hong Kong, China, October 2000), pages 387-395, Los Alamitos, 2000. IEEE Computer Society.
5. G. van den Bergen (2003), “*Collision Detection in Interactive 3D Environments*”. Morgan Kaufmann 2003.
6. D. Christianson, S. Anderson, L. He, D. Salesin, D. Weld, M. Cohen (1996). “*Declarative camera control for automatic cinematography*”. Thirteenth National Conference on Artificial Intelligence, 148-155.
7. N. Courty, E. Marchand (2001). “*Computer animation: a new application for image-based visual servoing*”. IEEE Int. Conf. on Robotics and Automation, Volume 1, pages 223–228, Seoul, South Korea, Mai 2001.
8. S.M. Drucker, D. Zeltzer (1995). “*CamDroid: A system for implementing intelligent camera control*”. P. Hanrahan and J. Winget, editors, 1995 Symposium on Interactive 3D Graphics, pages 139-144. ACM SIGGRAPH, Apr. 1995. ISBN 0-89791-736-7.
9. M. Gleicher, A. Witken (1992). “*Through-the-Lens Camera Control*”. Computer Graphics, 26(2): 331-340.
10. H.H. Gonzalez-Banos, C.Y. Lee, and J.-C. Latombe (2002). “*Real-Time Combinatorial Tracking of a Target Moving Unpredictably Among Obstacles*”. Proc. IEEE Int. Conf. on Robotics and Automation, 1683-1690, Washington D.C., May 2002.

11. N. Halper, P. Olivier (2000). "*Camplan: A Camera Planning Agent*". Smart Graphics. Papers from the 2000 AAAI Spring Symposium (Stanford, March 20-22, 2000), pages 92-100, Menlo Park, 2000. AAAI Press.
12. N. Halper, R. Helbing, T. Strothotte (2001). "*Computer Games: A Camera Engine for Computer Games*". Computer Graphics Forum Volume 20, Issue 3.
13. A. Hanson, E. Wernert (1997). "*Constrained 3D Navigation with 2D Controllers*". IEEE Visualisation, pages 175-182.
14. Hanson, A., E. Wernert, S. Hughes (1999). "*Constrained navigation environments*". Scientific Visualization: Dagstuhl '97 Proceedings, H. Hagen, G.M. Nielson, and F. Post, Editors. 1999, IEEE Computer Society Press. p. 95-104.
15. L.-W. He, M.F. Cohen, D.H. Salesin (1996). "*The Virtual Cinematographer: a Paradigm for Automatic Real-Time Camera Control and Directing*". Proceedings of ACM SIGGRAPH'96, pp. 217-224, 1996.
16. L. Kavraki, J.C. Latombe (1994). "*Randomized preprocessing of configuration space for fast path planning*". Proc. IEEE Int. Conf. on Robotics and Automation, 1994, pp. 2138-2145.
17. L. Kavraki, P. Švestka, J. Latombe, and M. Overmars. (1996). "*Probabilistic Roadmaps for Path Planning in High-Dimensional Configuration Spaces*". IEEE Transactions on Robotics and Automation, vol. 12, no. 4, pp. 566-580.
18. S.M. LaValle, H.H. Gonzalez-Banos, C. Becker, J.-C. Latombe (1997). "*Motion Strategies for Maintaining Visibility of a Moving Target*". Proceedings of the 1997 IEEE International Conference on Robotics and Automation, pages 731-736.
19. S. LaValle, J. Kufner (2001). "*Rapidly-exploring random trees: Progress and prospects*", in Algorithmic and Computational Robotics: New Directions (B. Donald, K. Lynch, and D. Rus, eds.), pp. 45-59, A.K. Peters, 2001.
20. T.Y. Li (1999). "*An Auto-Navigation System for Virtual Factories*". Proceedings of 1999 Automation Technology Conference, Chia-I, Taiwan.
21. T.Y. Li, J.M. Lien, S.Y. Chiu, T.H. Yu (1999). "*Automatically Generating Virtual Guided Tours*". Proceedings of the Computer Animation '99 Conference, Geneva, Switzerland, pp. 99-106, May 1999.
22. J. Mackinlay, S. Card, G. Robertson (1990). "*Rapid controlled movement through a virtual 3d workspace*". Computer Graphics (SIGGRAPH '90 Proceedings), pages 171-176, July 1990.
23. E. Marchand, N. Courty (2000). "*Image-based virtual camera motion strategies*". Graphics Interface Conference, GI2000, pages 69-76, 2000.
24. D. Nieuwenhuisen, M.H. Overmars (2003). "*Motion Planning for Camera Movements in Virtual Environments*". Proc. IEEE Int. Conf. on Robotics and Automation 2004, to appear.
25. M.H. Overmars (1992). "*A random approach to motion planning*". Technical Report RUU-CS-92-32, Dept. Comput. Sci., Utrecht Univ., Utrecht, the Netherlands, 1992.
26. C.B. Phillips, N.I. Badler, J. Granieri (1992). "*Automatic viewing control for 3D direct manipulation*". M. Levoy and E. E. Catmull, editors, Proceedings of the 1992 Symposium on Interactive 3D Graphics, pages 71-74, Cambridge, MA, Mar.-Apr. 1992. ACM Press.